Journal of Cerebral Blood Flow & Metabolism (2010) 30, 816–826

www.jcbfm.com

Simultaneous estimation of input functions: an empirical study

R Todd Ogden[1,2,3], Francesca Zanderigo[2], Stephen Choy[2], J John Mann[2,3] and Ramin V Parsey[2,3]

[1]*Department of Biostatistics, Columbia University, Mailman School of Public Health, New York, New York, USA;* [2]*Department of Molecular Imaging and Neuropathology, New York State Psychiatric Institute, New York, New York, USA;* [3]*Department of Psychiatry, Columbia University, College of Physicians and Surgeons, New York, New York, USA*

In neuroreceptor mapping, methods for the estimation of distribution volume require determination of a metabolite-corrected arterial input function. In application, this may be accomplished by collecting arterial blood samples during scanning, adjusting these measurements according to a separate metabolite analysis, and then modeling the resulting concentration data. Although many groups do this routinely, it is invasive and requires considerable effort. Furthermore, both the plasma and the metabolite data are noisy, and thus estimation of kinetic parameters can be affected by this variability. One promising alternative to full-input function modeling is the simultaneous estimation (SIME) approach, in which kinetic parameters and common input function parameters are estimated using results obtained from several regions at once. We investigate the performance of this approach on data from four different radioligands, using various kinetic models, comparing the results with those obtained by estimation using full-input function modeling. Results indicate that SIME provides a promising alternative for all the radioligands considered.
Journal of Cerebral Blood Flow & Metabolism (2010) **30,** 816–826; doi:10.1038/jcbfm.2009.245; published online 9 December 2009

Keywords: neuroreceptor mapping; simulated annealing

Introduction

Positron emission tomography (PET) is used for quantifying the distribution of various proteins in the brain. In such studies, the method used for the estimation of distribution volume that involves the fewest assumptions requires determination of a metabolite-corrected arterial input function to be used in kinetic modeling (or in one of its alternatives) of each time–activity curve (TAC) in the brain.

In practical application, this input function is typically determined by collecting blood samples at several time points from the subject's radial artery during PET imaging, and by measuring total concentration of the radioactive compound in each sample. In addition, during PET image acquisition, several blood samples are subjected to a metabolite analysis to determine the fraction of unmetabolized parent compound over a period of time. The metabolism function may then be estimated by fitting a model to the metabolite data and thereafter applied to 'correct' the arterial concentration data for the metabolite portion. The input function may then be estimated by fitting another model to the metabolite-corrected concentration data and then 'plugged in' to perform kinetic modeling of each brain TAC.

Although arterial sampling is performed routinely by many groups, it is invasive and requires considerable effort. Furthermore, both the plasma and the metabolite data are noisy, and thus estimation of kinetic parameters will be affected by this variability. For these reasons, much work has been carried out to eliminate the need for arterial sampling, such as development of 'reference tissue' methods that use only imaging data to estimate kinetic parameters (see, e.g., Gunn *et al*, 2001). These require identification of a region that is devoid of the receptor of interest, and allow only estimation of $BP_{ND} = f_{ND}BP_F$, where f_{ND} is the free fraction of the radioligand in the nondisplaceable compartment and $BP_F = B_{max}/K_D$,

Correspondence: Professor RT Ogden, Department of Biostatistics, Columbia University, 722 W. 168th St., 6th floor, New York, NY 10032, USA.
E-mail: todd.ogden@columbia.edu
This work was partially supported by United States Public Health Service grants MH40695 and MH62185. Funding for studies was also provided by MH062185-08.
Received 3 July 2009; revised 7 October 2009; accepted 27 October 2009; published online 9 December 2009

where B_{max} is protein density and K_D the dissociation constant.

Several methods for recovering the (metabolite-corrected) input function from PET data have also been developed. Such methods allow for the estimation of V_T and BP_P ($BP_P = f_P BP_F$, where f_P is the free fraction of the radioligand in the plasma) with little or no blood sampling during PET scanning. One general approach is to identify voxels in the PET image that correspond to arteries and to use data in these voxels to estimate the input function. One possibility for this approach is to define a region of interest (ROI) over a carotid artery defined in PET images (Chen *et al*, 1998; Sanabria-Bohorquez *et al*, 2003) or through magnetic resonance imaging coregistration (Litton, 1997). Alternatively, cranial blood pools can be identified using factor analysis (Wu *et al*, 1995) or independent component analysis (Naganawa *et al*, 2005; Su *et al*, 2005) on voxel data. Using arterial ROIs can be especially prone to partial volume effects because of the small diameter of the artery and spillover from the tissue. Factor analysis and independent component analysis can have noisy voxel data and intraframe motion. Furthermore, a fast acquisition protocol is required to accurately capture the shape of the peak for all the aforementioned strategies. We further note that although these techniques can recover an input function, the recovered input function will not be metabolite corrected.

A second general approach to extracting the input function from PET data is a population-based approach that assumes a common input function shape across subjects. A standard curve is created by normalizing input functions measured from arterial samples obtained from a large population. Input functions for future subjects are based on the standard curve and adjusted by a scaling factor derived from arterial samples (Brock *et al*, 2005; Takikawa *et al*, 1993), the net injected dose divided by body mass (Tsuchida *et al*, 1999), or from activity in the cerebellum (Bentourkia, 2006). To date and to our knowledge, this approach has only been studied for [^{18}F]fluoro-2-deoxyglucose ([^{18}F]FDG). In addition, it should be noted that before this approach can be adopted for any radioligand, many subjects would first have to be scanned with complete arterial sampling. Moreover, in subsequent comparison of groups, it would be necessary to assume that input functions do not differ among groups. Such an approach would not be valid in pre/postimaging studies in which the challenge will likely change the input function.

Another general alternative to recovering the input function from PET data may be termed 'the simultaneous estimation (SIME) approach,' as it seeks to estimate input function parameters simultaneously with kinetic parameters from several ROIs. This is accomplished by incorporating the input function parameters into the objective function to be optimized while modeling several ROI data sets simultaneously, thus 'borrowing strength' across ROIs to recover the input function common to all ROIs. We emphasize the fact that the SIME approach does not obviate the need to draw any blood during scanning; to ensure model identifiability, at least one measurement must be made on arterial or perhaps on venous plasma concentration. This is due to the nature of the method: there exist equivalent solutions for the input function that differs only by a scaling factor. The primary drawback of this approach is that the large number of parameters (input function parameters, plus kinetic parameters for each ROI) leads to a high-dimensional space over which to optimize. Standard estimation algorithms such as nonlinear least squares are not always suitable for finding a global optimum in a high-dimensional space, because they can easily get 'stuck' in the local optima, and thus fail to reach the global optimum. As a more robust alternative to nonlinear least squares, Wong *et al* (2002) applied the simulated annealing technique and showed its feasibility in simulated cardiac dynamic SPECT (single photon emission computed tomography)^{99m}Tc-teboroxime studies.

Other strategies similarly use multiple ROIs to recover the input function. Guo *et al* (2007) adopted the SIME approach augmented with an image-derived input function for early time frames and three blood samples at later time frames. Riabkov and Di Bella (2002) examined three algorithms that use only brain TACs to estimate physiologic parameters. By avoiding the use of a parameterized input function as in SIME, the algorithms prevent the need for any *a priori* knowledge of the input function. However, the authors acknowledge that including such knowledge is likely to produce better accuracy. A related method is proposed by Naganawa *et al* (2008), in which a geometric approach is adopted to estimate the integrated plasma TAC for use in graphical analysis.

Most of the proposed SIME methods require more than one blood sample to scale the recovered input function. The notable exceptions include some population-based (Bentourkia, 2006; Brock *et al*, 2005; Tsuchida *et al*, 1999; Wakita *et al*, 2000) and image-derived methods (Litton, 1997; Naganawa *et al*, 2005; Su *et al*, 2005), although as mentioned above, image-derived methods do not allow for metabolite correction. If multiple samples must be drawn from an artery, then, at least in terms of subject comfort and cost, there is no appreciable benefit over inserting an arterial catheter. One strategy that is less invasive is to replace arterial sampling with venous sampling. In some instances, this substitution is essentially equivalent, as is the case of [^{18}F]FDG and [^{18}F]Altanserin at late times (Bodvarsson and Mørkebjerg, 2006; Brock *et al*, 2005; Chen *et al*, 1998; see also Phelps *et al*, 1979). Similar equivalence of venous samples with arterial samples has been shown for other tracers, such as [^{11}C]*N*-methylspiperone ([^{11}C]NMSP) (Wong *et al*, 1986, 1997), but this

determination must be made separately for each candidate tracer.

Our motivation for investigating methods for determining an input function from the imaging data is threefold. Of primary importance, it can be used as a full replacement of arterial sampling and eliminate the drawbacks outlined previously. Second, it can be used as a backup in case arterial data are corrupted, lost, or unavailable. Finally, such a method can be applied routinely to studies that have complete arterial data to identify potential problems, either with the data or with the modeling.

Previous work on SIME by other authors showed the feasibility of the method using simulated data (Wong *et al*, 2002; Riabkov and Di Bella, 2002) or a relatively small number of [^{18}F]FDG scans (e.g., Wong *et al*, 2001). Typically, simulation studies are idealized in that the blood data are assumed to be error free. [^{18}F]FDG studies also are particularly well suited for SIME because the blood data do not need to be metabolite corrected, a step that can often introduce significant variability to the blood data and modeling. In addition, all previous work has relied on multiple blood samples collected during the scan, which, as mentioned earlier, is not optimal in terms of subject comfort and the number of technicians required for data acquisition.

In this study, we investigate the performance of SIME for four different tracers while taking into account the noise in plasma analysis, in metabolite analysis, and in TAC data, allowing only one blood sample per study. The SIME approach using the simulated annealing algorithm is applied to human data, each with complete arterial data, to compare the resulting estimated kinetic parameters directly. The radioligands considered are as follows: [^{11}C]-3-amino-4-(2-dimethylaminomethylphenylsulfanyl) benzonitrile ([^{11}C]DASB); *N*-(2-(4-(2-methoxyphenyl)-1-piperazinyl)ethyl)-*N*-(2-pyridinyl) cyclohexane carboxamide ([^{11}C]WAY); [^{18}F]FDG; and [*N*-methyl-C-11]-2-(4-methylamino-phenyl)-6-hydroxybenzothiazole ([^{11}C]BTA).

Materials and methods

Data Acquisition and Analysis

Data obtained from large past and ongoing studies were used for this study. Table 1 presents the radioligands used, number of subjects, scanning duration, ROIs considered, arterial sampling and metabolite correction protocols, and modeling methods. The Institutional Review Board of the New York State Psychiatric Institute approved the protocol. Subjects gave written informed consent after an explanation of the study.

Table 1 Data acquisition and analysis protocol for the radioligands under investigation

Radio-ligand	*Kinetic model*	*No. of subjects*	*Scan duration (mins)*	*Frame durations*	*No. of met pts*	*No. of plas pts*	*Plasma time points (mins)*	*Brain regions used in SIME*	*Metabolite model*
[^{11}C]DASB	1T	25	120	20 secs × 3, 1 mins × 3, 2 mins × 3, 5 mins × 2, 10 mins × 10	6	31	0.17, 0.33, 0.5, 0.67, 0.83, 1, 1.17, 1.33, 1.5, 1.67, 1.83, 2, 2.33, 2.67, 3, 3.33, 3.67, 4, 6, 8, 12, 16, 20, 30, 40, 50, 60, 70, 80, 90, 100	GCER, MID, AMY, DCA, HIP, TEM, VST	Damped biexponential
[^{11}C]WAY	2TC	7	110	20 secs × 3, 1 mins × 3, 2 mins × 3, 5 mins × 2, 10 mins × 9	6	31	0.17, 0.33, 0.5, 0.67, 0.83, 1, 1.17, 1.33, 1.5, 1.67, 1.83, 2, 2.33, 2.67, 3, 3.33, 3.67, 4, 6, 8, 12, 16, 20, 30, 40, 50, 60, 70, 80, 90, 100	WCER, HIP, TEM, OCC, ACN	Hill
[^{18}F]FDG	2Tirr	9	60	15 secs × 8, 30 secs × 6, 1 mins × 5, 5 mins × 4, 10 mins × 3	—	14	0.17, 0.33, 0.5, 0.67, 0.83, 1, 1.17, 1.33, 1.5, 2, 5, 20, 40, 60	CER, CIN, HIP, PFC, PIP	—
[^{11}C]BTA	2T	10	90	20 secs × 3, 1 mins × 3, 2 mins × 3, 5 mins × 2, 10 mins × 7	7	30	0.17, 0.33, 0.5, 0.67, 0.83, 1, 1.17, 1.33, 1.5, 1.67, 1.83, 2, 2.33, 2.67, 3, 3.33, 3.67, 4, 6, 8, 12, 16, 20, 30, 40, 50, 60, 70, 80, 90	CER, CIN, HIP, PFC, PIP	Hill

ACN, anterior cingulate; AMY, amygdala; [^{11}C]BTA, [*N*-methyl-C-11]-2-(4-methylamino-phenyl)-6-hydroxybenzothiazole; CER, cerebellum; CIN, cingulate; [^{11}C]DASB, [^{11}C]-3-amino-4-(2-dimethylaminomethylphenylsulfanyl) benzonitrile; DCA, dorsal caudate; GCER, gray matter cerebellum; HIP, hippocampus; met, metabolite; MID, midbrain; OCC, occipital lobe; PFC, prefrontal cortex; PIP, parahippocampal gyrus; plas, plasma; pt, point; SIME, simultaneous estimation; TEM, temporal lobe; VST, ventral striatum; WCER, white matter cerebellum; 1T, one tissue; 2T, two tissue; 2Tirr, two-tissue irreversible; [^{18}F]FDG, [^{18}F]fluoro-2-deoxyglucose; [^{11}C]WAY, *N*-(2-(4-(2-methoxyphenyl)-1-piperazinyl)ethyl)-*N*-(2-pyridinyl) cyclohexane carboxamide.
The brain regions listed are the regions included for SIME.

Brain Regions

For SIME to perform well, regions used for the estimation of the input function should have distinct kinetic behavior (Wong *et al*, 2002). The regions used in this study were chosen to represent a broad range of kinetic behavior for each radioligand. Regions of interest were traced on individual magnetic resonance imaging on the basis of brain atlases (Duvernoy, 1991; Talairach and Tournoux, 1988) and published reports (Kates *et al*, 1997; Killiany *et al*, 1997) and were verified by a neuroanatomist.

Modeling of Time–Activity Curve Data

The kinetic behavior of each radioligand considered may be described by any of a variety of models. A parametric form is assumed for the metabolite-corrected arterial input function (in our application, a sum of three exponentials after the peak). For any kinetic model, the expression for the concentration in region i is given by

$$f_\theta(t;\, R_i,\, L_i) = \sum_{k=1}^{K} L_{ik} \mathrm{e}^{-R_{ik}t} \otimes C_p(t;\, \theta)$$

where the input function C_p $(t;\, \theta)$ depends on a set of parameters θ, K is the number of tissue compartments, and the macroparameters $L_i = (L_{i1}, \ldots, L_{iK})$ and $R_i = (R_{i1}, \ldots, R_{iK})$ depend on the rate constants of the particular compartmental structure (Gunn *et al*, 2001; Ichise *et al*, 2001). We consider three versions of this general model: a one-tissue model for [^{11}C]DASB, a two-tissue model (2T) for [^{11}C]BTA, a 2T model constrained to have the K_1/k_2 ratio equal that of the reference region (2TC) for [^{11}C]WAY, and a 2T irreversible model (2Tirr) for [^{18}F]FDG.

When arterial data are available, we estimate θ from the metabolite-corrected arterial data, and substitute the resulting estimate $\hat{\theta}$ into the expression above. The ROI-specific parameters would then typically be estimated one ROI at a time by minimizing for each i:

$$\sum_{j=1}^{n} w_j (Y_{ij} - f_{\hat{\theta}}(t_j;\, R_i,\, L_i))^2$$

using an iterative nonlinear least squares algorithm over all choices of L_i and R_i, where Y_{ij} is the measured concentration of the radioligand in region i at time t_j and $(w_1, \ldots, w_n)$ a set of known weights. In our application, the weights are set to the frame duration.

Simultaneous Estimation

The general SIME approach exploits the fact that the parameters for the input function are common across all ROIs. For N regions, the combined objective function becomes

$$\Phi(\theta, L_1, \ldots, L_N, R_1, \ldots, R_N) = \sum_{i=1}^{N} \sum_{j=1}^{n} w_j (Y_{ij} - f_\theta(t_j;\, R_i,\, L_i))^2 + \sum_{\ell=1}^{L} v_\ell (P_\ell - C_p(s_\ell;\, \theta))^2 \quad (1)$$

for plasma samples $P_1, \ldots, P_L$ taken at time points $s_1, \ldots, s_L$, respectively. The last term in the above expression helps ensure agreement of the estimated input function with any blood samples collected. In our application, following Wong *et al* (2002), the weights for this term $(v_1, \ldots, v_L)$ were set to 100. For our data (measured in μCi/cm^3), this value was high enough to ensure that the estimated input function passes through the plasma data. For data measured in different units, this choice would need to be revisited.

Arterial Sampling and Metabolite Correction

In our implementation of SIME, we set $L = 1$ in Equation (1), i.e., using only one arterial sample. The concentration at this point was corrected for metabolite on the basis of metabolite analysis of blood drawn at the same time as the single plasma sample.

In our existing data, there are generally six blood samples collected for metabolite analysis in each study. For application of the SIME described in this study, we considered only sampling plasma at time points for which we also had metabolite data.

Simulated Annealing

The objective function Equation (1) can be quite challenging to minimize. There can be numerous local minima due in part to the high dimensionality of the parameter space. For estimating θ accurately, it would be natural to consider many regions at once, but this will have the effect of increasing the dimensionality of the objective function even further, making it still more difficult to locate a global minimum. Standard nonlinear least square algorithms are not guaranteed to find the global minimum and often get trapped in local minima.

Simulated annealing was developed as a robust optimization algorithm (Kirkpatrick *et al*, 1983). Its name comes from the analogy of annealing two materials by heating to a high temperature and slowly cooling. At high temperatures, thermal fluctuation prevents the formation of metastable energy states and, given a sufficiently long cooling schedule, the material will settle into a state of minimal energy—a perfect crystal. Following this analogy, in the simulated annealing algorithm, the set of parameters is treated as a state and the objective function Φ as the energy of the state. The algorithm travels iteratively through parameter space by randomly choosing a new 'candidate state' (determined by a new set of parameters) at each step. The new state is accepted with probability given by the Metropolis criterion:

$$P(\Delta\Phi) = \begin{cases} 1, \text{ if } \Delta\Phi \leq 0 \\ \mathrm{e}^{-\frac{\Delta\Phi}{T}}, \text{ otherwise} \end{cases}$$

where $\Delta\Phi$ is the decrease in the value of the objective function that would result from moving to the new state and T the temperature of the system, which is gradually decreased at each step. At high temperature (corresponding to early steps in the algorithm), the Metropolis criterion allows the algorithm to escape local minima by sometimes accepting 'uphill' movements. As the temperature decreases, the algorithm becomes gradually more selective for 'downhill' movements.

For this study, the simulated annealing algorithm was implemented similar to that described by Wong *et al* (2002). The initial temperature was set at $T = 100$, which is higher than Wong's starting temperature considering he multiplies T by the Boltzmann constant. At the initial temperature, $P(\Delta\Phi)$ is typically close to 1. Although this initial starting temperature leads to a considerably slower convergence than Wong's, it does allow for a more extensive search. Starting values for the parameters are chosen randomly, constrained according to limits derived from results of modeling data with full blood modeling. In particular, each parameter is constrained to be positive, and the upper limit for each parameter was set considerably higher than any of the corresponding estimated parameters. The choice of limits does not appreciably affect the results, because as part of the simulated annealing algorithm (see below) these limits are iteratively reduced until convergence. For each iteration, the candidate state is calculated by perturbing one current parameter value based on a uniform distribution with a range that is specific to each parameter. This range is set to the limits described above for the first set of iterations and is gradually tightened (see below) as the algorithm progresses. The candidate parameter vector is 'accepted' (and thus replaces the previous parameter values) with probability $P(\Delta\Phi)$. This perturbation and acceptance/rejection step is repeated 20 times for each parameter, and the algorithm works through each parameter in turn. After one round of searches through all the parameters, the algorithm adjusts the vector of ranges so that the acceptance rate of new candidates is $\sim 50\%$. After 10 rounds of adjusting the range vector, the current value of the parameters is stored as an intermediate solution and the temperature is decreased by a factor of 0.8. The algorithm continues until the objective function evaluated at the last four intermediate solutions differs by $< 10^{-5}$. The maximum number of iterations was set at 5×10^6, which was high enough so that the algorithm did not prematurely terminate. The algorithm was coded in Matlab 7.1 (Mathworks, Natick, MA, USA) and run on an Intel Xeon workstation (Intel, Santa Clara, CA, USA) (2.50-Ghz CPU, 3 GB RAM). Computational time for one study was ~ 20 mins when seven regions were used for optimization.

Outcome Measures

A general outcome measure of kinetic modeling is total volume of distribution V_T, defined as $V_T = \sum_{k=1}^{K} L_k / R_k$. For the 2Tirr model (used for the FDG data), the outcome measure used in comparisons is simply L_K, which is proportional to cerebral metabolic rate for glucose utilization (Gunn *et al*, 2001).

Determination of Optimal Blood Sampling Time

To determine the optimal time at which a single arterial sample may be drawn, we estimated outcome measures for each ROI for each subject by two methods: (1) using all available arterial data (including both the plasma concentration measurement and the metabolite analysis) and (2) applying SIME without performing blood volume correction on TAC data using only a single blood sample (consisting of both plasma concentration and metabolite analysis). This was repeated for each point for which these data are available and the optimal time was chosen to be the one that has the closest agreement between estimates (determined by lowest mean percentage difference) computed both ways. Subsequent SIME analysis was conducted using only the times determined to be optimal.

Blood Volume Correction

When modeling dynamic PET data, we note that the Y_{ij} values in Equation (1) represent measurements of the concentration of the radioligand in the given brain region, but in fact they also include some concentration in the blood vasculature. When measurements on the total concentration in the plasma are available, the Y_{ij} values can be 'corrected' for vascular contribution by subtracting some fixed multiple of the total concentration curve or by working the vascular contribution into subsequent modeling (Frankle *et al*, 2006; Mintun *et al*, 1984). A limitation of the SIME approach is that it only allows for estimation of the (metabolite-corrected) plasma function. Thus, without further data (or assumptions) such a correction based on total plasma concentration is not possible.

To investigate how much the lack of vascular correction may contribute to the disagreement in the two estimation strategies (SIME and full blood modeling), we considered the following three different possibilities: (1) no vascular correction, (2) vascular correction within SIME using the metabolite-corrected plasma function estimated at each iteration (i.e., correcting the TACs at each iteration by subtracting a fixed multiple of the current estimate of the metabolite-corrected plasma function), and (3) 'population-based' vascular correction using a total (uncorrected for metabolites) plasma function that is determined for each radioligand by averaging such functions from many subjects with full blood data available.

Application of Simultaneous Estimation in Constrained Kinetic Modeling

As stated earlier, we used a 2T model for the [^{11}C]WAY data with the K_1/k_2 ratio for each region constrained to be equal to that of the reference region (cerebellar white matter; Parsey *et al*, 2005) that is fit with a one-tissue model. When applying the SIME approach to such data, the input function is first estimated using all regions and the same model. Once the input function has been estimated, a one-tissue model is fit to the reference region to estimate K_1 and k_2, then the appropriately constrained model is fit to all other ROIs using the estimated input function.

Performance Indices

For each region and for each subject, outcome measures of interest were estimated using both kinetic modeling with the full-input function and the SIME approach using

simulated annealing and blood data collected only at the 'optimal' arterial sampling point. Agreement between each SIME approach and the full-input function modeling estimates was evaluated by calculating the percentage difference (the absolute difference of the two estimates divided by their average), a regression analysis with SIME estimates as the dependent variable and the full blood data as the independent variable, and the correlation coefficient.

Results

A summary of the results for all radioligands considered is provided in Table 2. To determine the effect of neglecting vascular correction, we also repeated the SIME algorithm for the other possibilities discussed in the 'Blood Volume Correction' section for each subject and for each radioligand. For [^{11}C]DASB, [^{11}C]WAY, and [^{11}C]BTA, the differences in the measures of agreement were small, and hence only the results for the analysis neglecting vascular correction are provided in the table. For the [^{18}F]FDG data, agreement between parameter estimates from SIME and those obtained using the full-input function depended on the vascular correction strategy, and therefore summaries are provided in the table for all these options. Agreement between outcome measures for [^{11}C]DASB, [^{11}C]WAY, and [^{11}C]BTA is displayed graphically, along with regression parameter estimates and correlation coefficients, in Figure 1. Similar plots are shown in Figure 2 for the three vascular correction options for [^{18}F]FDG.

Plots of individual input functions estimated both ways (SIME and using full blood data) are shown in

Table 2 Summary statistics of percentage difference for all radioligands of estimates using SIME with simulated annealing compared with those estimated with full-input modeling, computed over all subjects and regions

Ligand	*Vascular correction*	*Percentage difference*			*Optimal arterial sampling time (mins)*
		Mean	*s.d.*	*Max*	
[^{11}C]DASB	No	7.08	6.22	33.89	50
[^{11}C]WAY	No	24.17	19.69	72.91	20
[^{11}C]BTA	No	13.76	12.86	50.81	40
[^{18}F]FDG	No	24.66	8.35	35.16	
	Yes	11.39	4.91	19.73	40
	Pop	17.88	6.45	29.57	

SIME, simultaneous estimation; [^{18}F]FDG, [^{18}F]fluoro-2-deoxyglucose.
In the case of [^{18}F]FDG, results obtained with two vascular correction strategies are also reported: 'yes' in the vascular correction column indicates correction done using the (metabolite-corrected) plasma function; 'pop' refers to vascular correction done using the 'population-based' (total plasma concentration) curve estimated by averaging many subjects for whom plasma data are available. Columns refer to percentage difference (mean, s.d., and max). Optimal arterial sampling time is also included in the table.

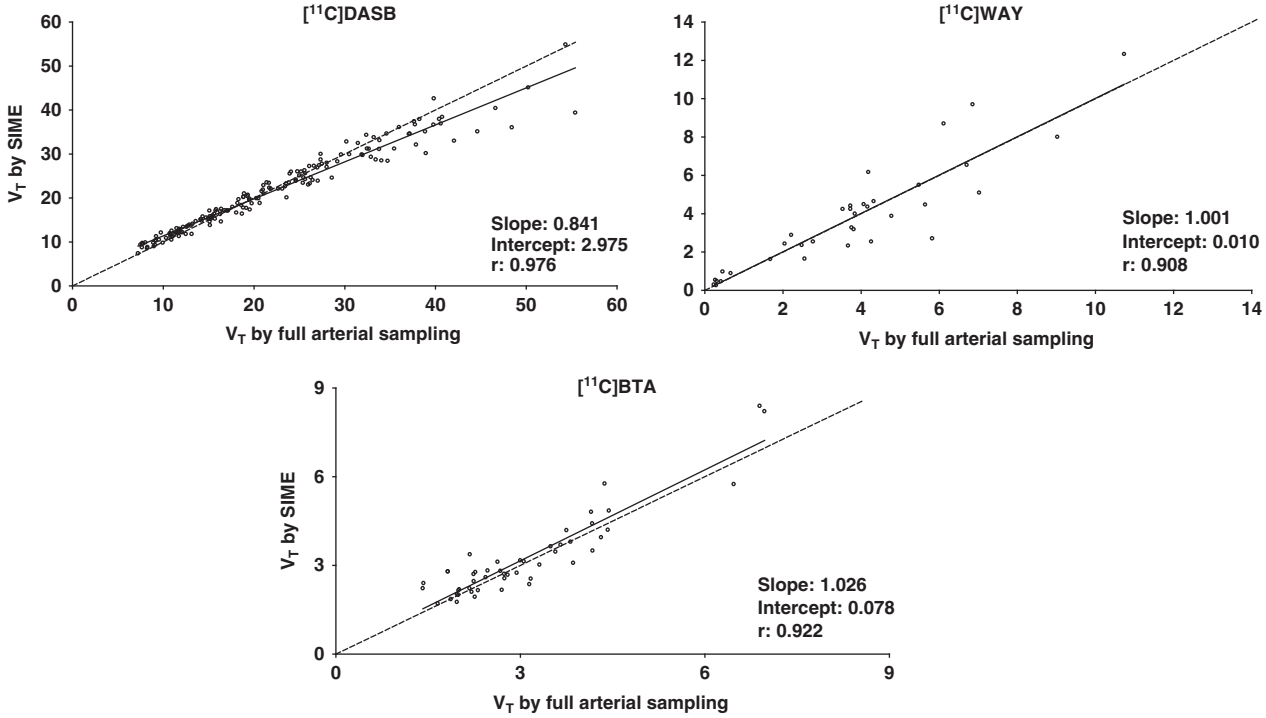

Figure 1 Scatterplots of estimated V_T values for [^{11}C]DASB, [^{11}C]WAY, and [^{11}C]BTA from SIME versus those estimated from full-input function modeling, for all subjects and all regions. The identity line (black dotted line) and the fitted regression line (black solid line) are included in each panel for reference. [^{11}C]BTA, [*N*-methyl-C-11]-2-(4-methylamino-phenyl)-6-hydroxybenzothiazole; [^{11}C]DASB, [^{11}C]-3-amino-4-(2-dimethylaminomethylphenylsulfanyl) benzonitrile; SIME, simultaneous estimation; [^{11}C]WAY, *N*-(2-(4-(2-methoxyphenyl)-1-piperazinyl)ethyl)-*N*-(2-pyridinyl) cyclohexane carboxamide.

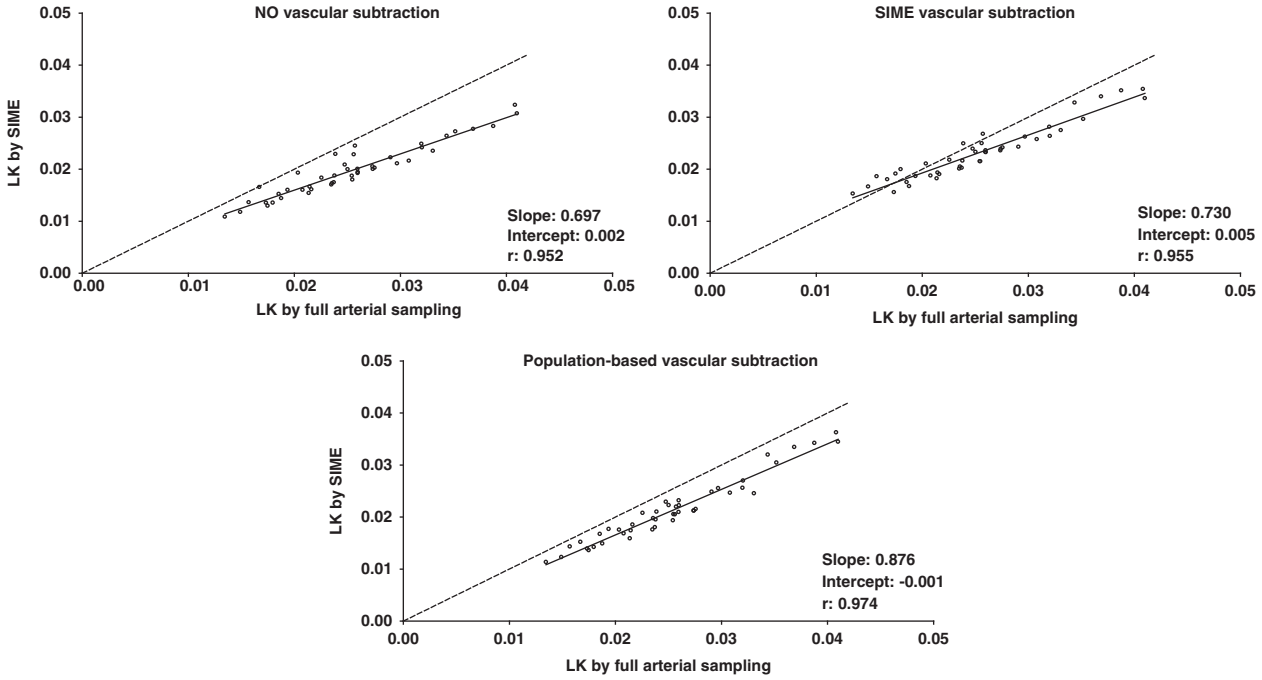

Figure 2 Scatterplots of estimated L_K values derived for [^{18}F]FDG for all the subjects using SIME with three different vascular correction strategies versus those from a full-input function modeling. The identity line (black dotted line) and the fitted regression line (black solid line) are included in each panel for reference. [^{18}F]FDG, [^{18}F]fluoro-2-deoxyglucose; SIME, simultaneous estimation.

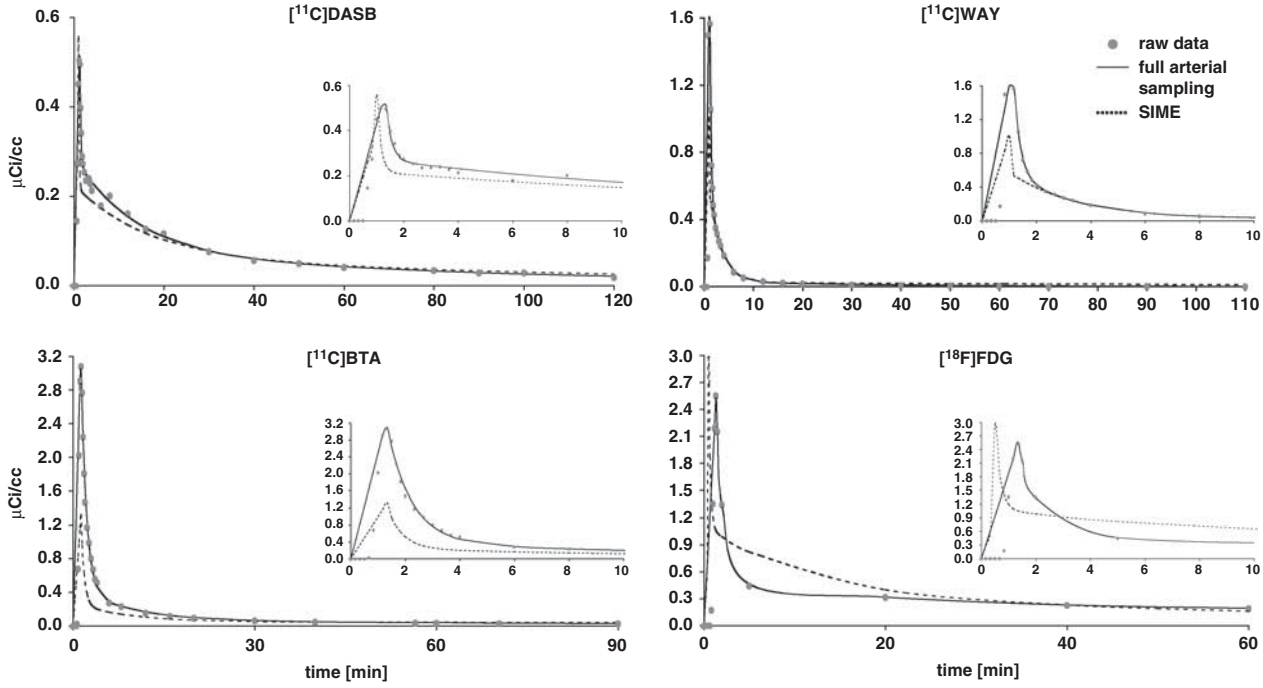

Figure 3 Plasma data with fits obtained from modeling all arterial samples (solid curve) and from SIME modeling (dotted curve) for representative studies for each ligand. Each plot contains an inset that 'zooms in' on the early part of the curve. [^{11}C]BTA, [*N*-methyl-C-11]-2-(4-methylamino-phenyl)-6-hydroxybenzothiazole; [^{11}C]DASB, [^{11}C]-3-amino-4-(2-dimethylaminomethylphenylsulfanyl) benzonitrile; [^{18}F]FDG, [^{18}F]fluoro-2-deoxyglucose; SIME, simultaneous estimation; [^{11}C]WAY, *N*-(2-(4-(2-methoxyphenyl)-1-piperazinyl)ethyl)-*N*-(2-pyridinyl) cyclohexane carboxamide.

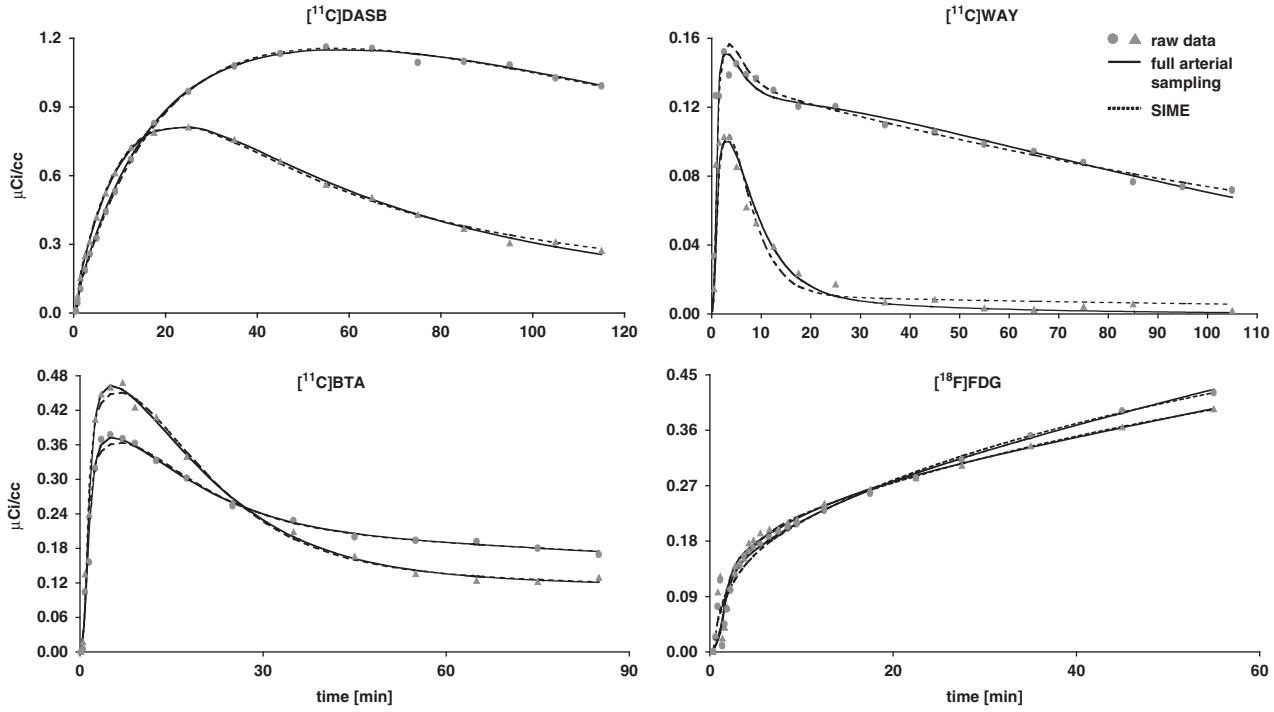

Figure 4 TAC data and fits obtained from both modeling strategies (solid curve for full arterial sampling, dotted curve for SIME) for two representative ROIs for one study for each ligand. SIME, simultaneous estimation; [^{11}C]BTA, [*N*-methyl-C-11]-2-(4-methylamino-phenyl)-6-hydroxybenzothiazole; [^{11}C]DASB, [^{11}C]-3-amino-4-(2-dimethylaminomethylphenylsulfanyl) benzonitrile; [^{18}F]FDG, [^{18}F]fluoro-2-deoxyglucose; [^{11}C]WAY, *N*-(2-(4-(2-methoxyphenyl)-1-piperazinyl)ethyl)-*N*-(2-pyridinyl) cyclohexane carboxamide.

Figure 3, with one representative study for each ligand considered. Agreement is generally good for the latter part of the data, with the most disagreement usually occurring near the early peak. The effect of using these different input functions on modeling TAC data can be seen in Figure 4. Although noticeable differences in input functions can be seen in Figure 3, the fits of the TAC data tend to be in greater agreement.

For all radioligands considered, there is fairly good agreement between the SIME estimates and those using full-input function modeling. For [^{11}C]DASB, the agreement is quite close, although Figure 1 indicates that there is some slight disagreement between full-input function modeling and SIME, with SIME tending to underestimate somewhat relative to full-input function modeling. For [^{11}C]WAY and [^{11}C]BTA, there is no noticeable relative bias, although the agreement is not as close as for [^{11}C]DASB.

For [^{18}F]FDG, the extent of the agreement of SIME with full-input function modeling depends on the strategy for vascular correction. For this radioligand, in contrast to the others considered in this study, simply neglecting the vascular contribution provided worse agreement than did the two approaches for accounting for it. The best agreement results from working the vascular contribution into the modeling.

To evaluate the amount of relative bias more objectively, we analyzed the data in a linear mixed effects model. Fixed effects were ROI and method (SIME or full arterial sampling), and random effects were subject and method nested within subject. Analysis was conducted on log-transformed data to stabilize the variance among regions and to allow for a proportional bias. In general agreement with conclusions that could be drawn from Figures 1 and 2, there is no significant bias for [^{11}C]DASB ($F = 0.031$; d.f. = 1, 24; $P = 0.86$), [^{11}C]WAY ($F = 0.11$; d.f. = 1, 6; $P = 0.76$), or [^{11}C]BTA ($F = 0.85$; d.f. = 1, 9; $P = 0.38$). For [^{18}F]FDG with the vascular correction worked into the modeling, the estimated relative bias (−7.57% for SIME relative to full arterial sampling) was significant ($F = 5.76$; d.f. = 1, 8; $P = 0.043$).

Discussion

Our results show that SIME with simulated annealing is a promising alternative to full arterial sampling for all the considered radioligands, as estimated outcome measures values recovered were comparable with values derived using full-input function modeling.

This consistency holds for [^{11}C]DASB, [^{11}C]WAY, and [^{11}C]BTA even when neglecting vascular correction to brain TACs. In the case of [^{11}C]DASB, this may be attributed to the fact that typical activity is much higher in brain regions than in the plasma: in the specific data set considered for this analysis, the tissue-to-whole-plasma activity ratios at 55 mins

after the radioligand injection across regions and subjects are in the range between 2.90 and 7.72, with mean and s.d. of 4.51 and 1.19, respectively. Owing to these high ratios, the vascular correction term, which is itself a small percentage of the input function, has a negligible effect on the brain TAC.

Blood volume correction has a more pronounced effect on brain TACs in [^{18}F]FDG studies. Either approach to vascular correction improved the recoverability of L_K as shown in Figure 2. The tissue-to-whole-plasma activity ratios obtained for [^{18}F]FDG at 55 mins after the radioligand injection across regions and subjects are lower than those for [^{11}C]DASB (range between 1.89 and 3.55, with mean and s.d. of 2.56 and 0.55, respectively). However, they are comparable with, if not higher than, those obtained at the same sampling time for [^{11}C]WAY and [^{11}C]BTA (range: 0.94 to 2.23; mean = 1.33 and s.d. = 0.43, for [^{11}C]WAY; range: 0.32 to 0.71; mean = 0.52 and s.d. = 0.13, for [^{11}C]BTA), for which the lack of vascular correction does not seem to have a significant effect on the SIME estimates. In this case, the tissue-to-whole-plasma activity ratios magnitude might not be the only reason for the different behavior of [^{18}F]FDG. The irreversible kinetics of this radioligand that, in contrast to the other considered radioligands, translates into increasing (instead of decreasing) tissue-to-whole-plasma activity ratios toward the end of the scan might be a factor. However, glucose metabolism was usually underestimated by simulated annealing relative to full-input function modeling, especially for the highest values.

Among the other alternatives to full arterial sampling that were considered for comparison was the strategy of using as each subject's input function some aggregate measure (in our application, the simple average) of such functions from historical studies using the same tracer. Although this may seem an effective strategy (in large part because of its simplicity), the obvious disadvantage is that using a single input function for all subjects neglects many potentially important factors, including differences in metabolism, volume of distribution, and injected dose among subjects (or even between scans at different times on the same subject).

As arterial sampling during a scan is considerably invasive and requires significant effort for the collection, analysis, and modeling of the resulting data, any reasonable alternative strategy that could at least reduce the amount of arterial blood required would represent a significant improvement. When estimating V_T is the objective, at least one blood sample must be collected to ensure identifiability. For the four ligands considered in this study, we have shown that a single arterial blood sample is sufficient for the estimation of V_T. This obviates the need for placement of an arterial catheter; instead a single arterial blood sample, similar to what is done for arterial blood gas determinations, may be used. This provides a significant reduction in the effort required for obtaining and analyzing multiple blood sampling samples, as well as in modeling the results, but it does not represent a great improvement in terms of patient comfort. Ideally, no arterial samples would be required at all, and the identifiability condition could be satisfied by collecting a single venous sample. Whether this is feasible depends on the properties of each ligand. For [^{18}F]FDG, for instance, we determined the optimal blood sampling time to be 40 mins after injection. For this ligand, we could replace the arterial sample with a venous one,

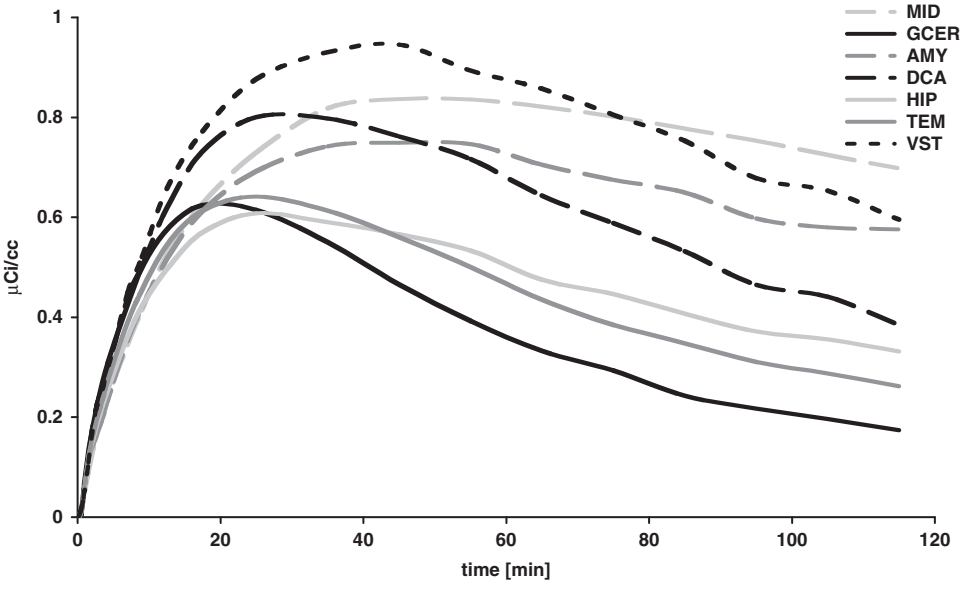

Figure 5 TAC data for the ROIs used in estimating the input function for DASB for a representative study. Regions were chosen so as to represent a range of kinetic behavior.

as at 40 mins after injection the ratio of venous plasma to arterial plasma radioactivity is close to one (Wakita *et al*, 2000). The relationship between arterial and venous data would have to be studied for each ligand before such a substitution could be made.

One potential drawback of SIME using only one blood sample is that it is highly dependent on that single measurement. Any error in that measurement will be reflected in the resulting estimation of kinetic parameters. (Of course, full-input modeling is also affected by such errors, but it is generally expected that these errors will tend to cancel each other out to some extent.) Thus, SIME will be most consistent with full-input function modeling for radioligands with relatively small errors in metabolite and plasma measurements.

Another factor in the performance of SIME is the dimensionality of the objective function. All other things being equal, it is reasonable to expect that simpler models will produce better results than more complex models. The success of [^{11}C]DASB may be due in part to our fitting of a kinetic model with only two parameters per region, creating a parameter space with roughly half the dimensionality of the 2T model.

Another factor that can affect the performance of SIME is the richness in the kinetic behavior of the regions used. In our application, we attempted to include regions with as wide a variety of kinetics as possible while avoiding regions that tend to be noisy. Recoverability of outcome measures may be improved with more regions of distinct kinetics. The variety in kinetic behavior seems to depend greatly on the radioligand. The TACs for the regions used in a typical [^{11}C]DASB study are shown in Figure 5, showing a reasonable range of kinetics. However, in our [^{11}C]WAY studies, although we had more than 30 regions available for analysis, we noted that many of these regions displayed very similar kinetics. Including regions with similar kinetic behavior would serve only to increase the dimensionality of the objective function without adding much useful information. In future work, we plan to consider the question of how best to select the total number of regions and which regions produce the best results for each ligand.

Although voxel data are readily available and can be expected to show a wide variety of kinetic behavior, it may be impractical to use voxel TACs in the SIME framework because of the very high noise in voxel-level data. Even if many voxels with distinct kinetics are available, the computational cost for simulated annealing would make analysis impractical. Voxel-level analysis could be accomplished in practice by using ROI data for estimation of the input function, and then by applying the resulting estimated input function for modeling all voxel TACs. In the absence of defined ROIs, a clustering algorithm could be applied to the voxel TACs, and then SIME applied to a subset of the clusters.

The analysis presented in this paper is based primarily on how well the results of SIME agree with those acquired using full-input modeling. As full-input modeling involves fitting many more blood samples than SIME, it can be expected to be more 'correct' and is generally regarded as the *de facto* 'gold standard.' In this study, we have found that there is general agreement between SIME and full-input modeling. Any discrepancy between these two results (in the case that full arterial data are available) would accordingly lead us to examine the data and the model fits and may reveal potential problems with the metabolite or the plasma data, or with model fits (e.g., one or more extreme outliers exerting undue influence).

Finally, it should be reiterated that simulated annealing has a rather high computation cost. For a typical [^{11}C]DASB study, computational time was $\sim$20 mins. Studies with more parameters took slightly longer. Optimizing the cooling schedule in simulated annealing, or using alternative programming languages has not been explored, and both strategies could potentially reduce computational cost.

Disclosure/conflict of interest

The authors declare no conflict of interest.

Acknowledgements

The authors are indebted to the employees of the Conte Center for the Neurobiology of Major Depression, the Kreitchman PET Center, and the Radioligand Laboratory for expert help.

References

Bentourkia M (2006) Kinetic modeling of PET-FDG in the brain without blood sampling. *Comput Med Imaging Graph* 30:447–51

Bodvarsson B, Mørkebjerg M (2006) *Analysis of Dynamic PET Data* Master's Thesis, Informatics and Mathematical Modelling Denmark: Technical University of Denmark, DTU

Brock CS, Young H, Osman S, Luthra SK, Jones T, Price PM (2005) Glucose metabolism in brain tumours can be estimated using [18F]2-fluorodeoxyglucose positron emission tomography and a population-derived input function scaled using a single arterialised venous blood sample. *Int J Oncol* 26:1377–83

Chen K, Bandy D, Reiman E, Huang SC, Lawson M, Feng D, Yun LS, Palant A (1998) Noninvasive quantification of the cerebral metabolic rate for glucose using positron emission tomography, 18F-fluoro-2-deoxyglucose, the Patlak method, and an image-derived input function. *J Cereb Blood Flow Metab* 18:716–23

Duvernoy H (1991) *The Human Brain. Surface, Three Dimensional Sectional Anayomy and MRI*. New York: Spring-Verlag Wien

Frankle WG, Slifstein M, Gunn RN, Huang Y, Hwang DR, Darr EA, Narendran R, Abi-Dargham A, Laruelle M (2006) Estimation of serotonin transporter parameters with 11C-DASB in healthy humans: reproducibility and comparison of methods. *J Nucl Med* 47:815–26

Gunn RN, Gunn SR, Cunningham VJ (2001) Positron emission tomography compartmental models. *J Cereb Blood Flow Metab* 21:635–52

Guo H, Renaut RA, Chen K (2007) An input function estimation method for FDG-PET human brain studies. *Nucl Med Biol* 34:483–92

Ichise M, Meyer JH, Yonekura Y (2001) An introduction to PET and SPECT neuroreceptor quantification models. *J Nucl Med* 42:755–63

Kates WR, Abrams MT, Kaugmann WW, Breiter SN, Reiss AL (1997) Reliability and validity of MRI measurement of the amygdala and hippocampus in children with fragile X syndrome. *Psychiatr Res Neuroimag* 75: 31–48

Killiany RJ, Moss MB, Nicholson T, Jolesz F, Sandor T (1997) An interactive procedure for extracting features of the brain from magnetic resonance images: the lobes. *Hum Brain Mapp* 5:355–63

Kirkpatrick S, Gelatt Jr CD, Vecchi MP (1983) Optimization by simulated annealing. *Science* 220:671–80

Litton JE (1997) Input function in PET brain studies using MR-defined arteries. *J Comput Assist Tomogr* 21:907–9

Mintun MA, Raichle ME, Kilbourn MR, Wooten GF, Welch MJ (1984) A quantitative model for the in vivo assessment of drug binding sites with positron emission tomography. *Ann Neurol* 15:217–27

Naganawa M, Kimura Y, Ishii K, Oda K, Ishiwata K, Matani A (2005) Extraction of a plasma time-activity curve from dynamic brain PET images based on independent component analysis. *IEEE Trans Biomed Eng* 52:201–10

Naganawa M, Kimura Y, Yano J, Mishina M, Yanagisawa M, Ishii K, Oda K, Ishiwata K (2008) Robust estimation of the arterial input function for Logan plots using an intersectional searching algorithm and clustering in positron emission tomography for neuroreceptor imaging. *Neuroimage* 40:26–34

Parsey RV, Arango V, Olvet DM, Oquendo M, Van Heertum R, Mann JJ (2005) Regional heterogeneity of 5-HT1A receptors in human cerebellum as assessed by positron emission tomography. *J Cereb Blood Flow Metab* 25:785–93

Phelps ME, Huang SC, Hoffman EJ, Selin C, Sokoloff L, Kuhl DE (1979) Tomographic measurement of local cerebral glucose metabolic rate in humans with (F-18)2-fluoro-2-deoxy-D-glucose: validation of method. *Ann Neurol* 6:371–88

Riabkov DY, Di Bella EVR (2002) Estimation of kinetic parameters without input functions: analysis of three methods for multichannel blind identification. *IEEE Trans Biomed Eng* 49:639–64

Sanabria-Bohorquez SM, Maes A, Dupont P, Bormans G, de Groot T, Coimbra A, Eng W, Laethem T, De Lepeleire I, Gambale J, Vega JM, Burns HD (2003) Image-derived input function for [11C]flumazenil kinetic analysis in human brain. *Mol Imaging Biol* 5:72–8

Su KH, Wu LC, Liu RS, Wang SJ, Chen JC (2005) Quantification method in [18F]fluorodeoxyglucose brain positron emission tomography using independent component analysis. *Nucl Med Commun* 26:995–1004

Takikawa S, Dhawan V, Spetsieris P, Robeson W, Chaly T, Dahl R, Margouleff D, Eidelberg D (1993) Noninvasive quantitative fluorodeoxyglucose PET studies with an estimated input function derived from a population-based arterial blood curve. *Radiology* 188:131–6

Talairach J, Tournoux P (1988) *Co-Planar Sterotactic Atlas of the Human Brain. Three Dimensional Proportional System: An Approach of Cerebral Imaging*. New York: Theime Medical Publisher

Tsuchida T, Sadato N, Yonekura Y, Nakamura S, Takahashi N, Sugimoto K, Waki A, Yamamoto K, Hayashi N, Ishii Y (1999) Noninvasive measurement of cerebral metabolic rate of glucose using standardized input function. *J Nucl Med* 40:1441–5

Wakita K, Imahori Y, Ido T, Fujii R, Horii H, Shimizu M, Nakajima S, Mineura K, Nakamura T, Kanatsuna T (2000) Simplification for measuring input function of FDG PET: investigation of 1-point blood sampling method. *J Nucl Med* 41:1484–90

Wong DF, Wagner HN, Tune LE, Dannals RF, Pearlson GD, Links JM, Tamminga CA, Broussole EP, Ravert HT, Wilson AA, Toung JKT, Malat J, Williams JA, O'Tuama LA, Snyder SH, Kuhar MJ, Gjedde A (1986) Positron emission tomography reveals elevated D_2 dopamine receptors in drug-naïve schizophrenics. *Science* 234:1558–63

Wong DF, Young D, Wilson PD, Meltzer CC, Gjedde A (1997) Quantification of neuroreceptors in the living human brain: III. D_2-like dopamine receptors: theory, validation, and changes during normal aging. *J Cereb Blood Flow Metab* 17:316–30

Wong KP, Feng D, Meikle SR, Fulham MJ (2001) Simultaneous estimation of physiological parameters and the input function—in vivo PET data. *IEEE Trans Inform Technol Biomed* 5:67–76

Wong KP, Meikle SR, Dagan F, Fulham MJ (2002) Estimation of input function and kinetic parameters using simulated annealing: application in a flow model. *IEEE Trans Nucl Sci* 49:707–13

Wu H-M, Hoh CK, Choi Y, Schelbert HR, Hawkins RA, Phelps ME, Huang S-C (1995) Factor analysis for extraction of blood time-activity curves in dynamic FDG-PET studies. *J Nucl Med* 36:1714–22